Effect of Ambient Turbulence on Trailing Vortices

Turgut Sarpkaya* and John J. Daly†
Naval Postgraduate School, Monterey, California

The effects of ambient turbulence (generated by a biplanar grid) on the migration and lifespan of trailing vortices are investigated in a towing tank through the use of two NACA-0012 foils moving at a constant angle of attack. The results show that the rise and demise of the vortices are controlled primarily by the rate of dissipation of the background turbulence. The integral scale of turbulence plays only a minor role. In both a quiescent or weakly-turbulent fluid the sinusoidal instability and in a fluid with stronger turbulence, the vortex bursting precedes the subsequent instability events which brings about the eventual destruction of the vortices. Both forms of the large scale instability are often accompanied by the roll of the vortex pair onto its side. Shear is not necessary for the roll but may enhance it under atmospheric conditions.

Nomenclature

$\mathcal{R}$ = aspect ratio of the wing
B = wing span
b_0 = initial vortex core spacing
c = chord length of the wing
d = width of a square bar in the grid
d_0 = initial depth of the vortex pair
H = vortex rise height
H^* = H/b_0, normalized migration height
L_{11} = integral scale of turbulence
M = mesh size of the grid
Re = Reynolds number
r_e = effective core radius
T^* = $V_0 t/b_0$, normalized time
t = time
U = model velocity
u = x component of velocity
v = y component of velocity
V_0 = $\Gamma_0/2\pi b_0$, initial mutual induction velocity
w = z component of velocity
x,y = coordinate axes
α = model angle of attack
Γ_0 = initial circulation of vortex
Δ = d_0/b_0
ϵ = rate of decay of turbulence energy
ϵ^* = $(\epsilon b_0)^{1/3}/V_0$, turbulence parameter
ν = kinematic viscosity of water
ρ = density of water

Introduction

THE migration and lifespan of the trailing vortices generated by a lifting surface are finite. The understanding of the demise mechanisms and the quantification of the downwash or upwash of the vortices during their lifespan in terms of the turbulence originating with or generated by the vortices (as a result of Helmholtz and Rayleigh instabilities during the roll up of the vortex sheets), the core size of the vortices (dependent on the roll-up process and the edge conditions of the foil), ambient turbulence of known intensity and integral scale (distinct from that originating with the vortex), stratification (due to temperature and/or salinity); ambient shear, and proximity effects (ground and free surface) have been the subject of entensive investigation during the past decade (see Refs. 1-5 and the references cited therein). The problem remains unresolved for a number of reasons: 1) The roll up of the vortex sheets is poorly understood. The distribution of the initial velocity and turbulence (say, at 10 chord lengths downstream from the lifting surface) that influence the core size and decay process cannot be changed independently. 2) Trailing vortices are extremely sensitive to disturbances created by even very small probes or bubbles (particularly in laboratory scales), making the measurement of the flow characteristics rather difficult. 3) There are also large-scale instabilities: Turbulence originating with or generated by the vortices slows down the migration of the vortex pair but does not directly destroy them: The vortex pair is destroyed by large scale instabilities (mutual induction instability[1] and/or vortex breakdown) and the subsequent instability events. 4) Scale effects are not easy to access. Even the highest Reynolds numbers, based on wing chord and reached in wind tunnels and towing tanks, are an order of magnitude lower than that what is possible for an aircraft. Fortunately, the existing data[4] tend to show that the Reynolds number effects are relatively small unless the large scale instabilities are absent. 5) The effects of core turbulence, ambient turbulence, shear, stratification, scale, and proximity are not linearly additive. 6) It is difficult to carry out systematic experiments even in a laboratory environment, partly because some parameters (such as the core size, velocity, and turbulence distributions in the core) cannot be varied systematically, and partly because the final stages of the demise of the vortices (due to Crow instability and/or vortex breakdown) can be quantified only subjectively. The time-honored diagnostic is the flow visualization. One assumes that the total diffusion of the dye initially seeding the core signals the end of the wake lifespan.

Most of the experimental data have been obtained in large-scale atmospheric tests using aircraft[6,7] or from vortex rings[3] migrating in a quiescent medium. Flight tests are usually limited in both quantity and quality of information that can be extracted because of the vagaries of atmospheric flow conditions.

The goal of the present study is to determine the effect of ambient turbulence (as distinct from the core turbulence in a quiescent medium) on the rise and demise of trailing vortices generated by two lifting surfaces in an unstratified medium and to obtain data against which the mathematical models may be checked. Clearly, the Reynolds number in our experiments is lower than one might expect for practical purposes, but the object of the investigation was understanding the evolution of the vortices under controlled conditions rather than to provide design data. It is hoped that such work will help in the interpretation of the full-scale results and provide inspiration for the development of improved mathematical models of the flow.

Reveived Oct. 22, 1986; revision received Dec. 2, 1986; presented as Paper 87-0042 at the AIAA 25th Aerospace Sciences Meeting, Reno, NV, Jan. 12-15, 1987. This paper is declared a work of the U.S. Government and is not subject to copyright protection in the United States.

†Professor, Mechanical Engineering, Member AIAA.
*Lieutenant, United States Navy, USS Peterson (DD-969).

Experimental Equipment and Procedures

The equipment used to generate the trailing vortices has been used extensively at this facility over the past three years.[4,8] Only the salient features, most recent modifications, and the adaptation for this work will be described here briefly.

Essentially, the system consists of a towing basin. The auxiliary components of the basin are the plumbing for water, turbulence management system, top and bottom carriages, velocity measuring system, and models.

Two parallel rails are mounted along the bottom of the tank. A carriage rides smoothly on these rails and provides the test body with a constant velocity through the use of an endless cable and a motor. The velocity of the model is measured and continuously monitored through the use of a magnetic linear displacement transducer.

The two rails, the carriages, and the filling pipes are located on or near the bottom of the basin and under a turbulence management system (a 1-in. thick polyurethane foam sandwiched between two perforated aluminum plates).

Models and Grids

Two rectangular foils (NACA-0012) were used in the present study (N-1 with $B=6.8$ in., $b_0=5.34$ in., and $c=3.50$ in., and N-2 with $B=4.50$ in., $b_0=3.53$ in., and $c=2.32$ in.). The interior of these models was hollowed and used as a dye reservoir to seed the vortex cores. The models are mounted on their bases by means of a thin streamlined aluminum bar with a cross section of a NACA-0006 foil and set at the desired angle of attack. As noted earlier, all models are pulled by means of a dc motor, pulley, and cable system at the desired speed (ranging from 0.8–4.0 ft/s).

Two biplanar grids were used in the experiments. They consisted of square plexiglass bars (3/8 x 3/8 in.). One layer was placed orthogonally on top of another so as to form a biplanar grid. The mesh sizes were $M=2.5$ and 3.5 in. The solidity of the grids, defined as $(2Md-d^2)/M^2$, was 0.28 and 0.20, respectively. In this paper, we report the results taken with the first grid although similar results were obtained with the second grid.

The test grid was attached to the top carriage and towed at desired speeds at x/M distances ahead of the model. It was made sure, through repeated experiments, that both the model and the grid ran smoothly, with very little or no velocity fluctuations. The mesh Reynolds number MU/ν ranged from 18,000–83,000.

Gid Generated Turbulence

A large number of grid-turbulence studies have been conducted in wind tunnels and in water flumes[9-14]. Measurements have shown that the grid-generated turbulence is only approximately isotropic with $u_2^2=u_3^2=0.83\ u_1^2$ for a uniform duct where u_1, u_2, u_3 are the longitudinal, lateral and vertical velocity components, respectively. In general, the mean-square velocity components of the turbulence decrease with the downstream distance according to the power law[12]

$$u_i^2/U^2=A_i(x/M)^{-n}\ (i=1\text{-}3) \tag{1}$$

where A_i are constants, M is the mesh size of the grid, U is the mean velocity of the ambient flow, and the power n ranges from 1.25–1.5. A careful examination of the existing data[9-14] has shown that (see Fig. 1) the most suitable values of A_i and n for the grid used in the present investigation are $A_1=0.05$ and $n=1.3$. Thus, one has

$$u_1^2/U^2=0.05(x/M)^{-1.3} \tag{2}$$

Consequently, twice the turbulent kinetic energy per unit mass becomes

$$q^2=(u_1^2+u_2^2+u_3^2)=1.71U^2(x/M)^{-1.3} \tag{3}$$

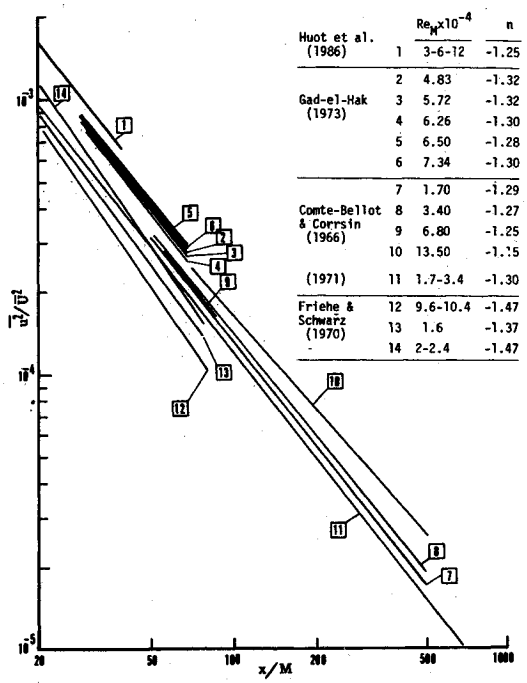

Fig. 1 Comparison of turbulence models.

The dissipation rate ϵ of the grid-generated turbulence per unit mass is defined as

$$\epsilon=-\frac{1}{2}\frac{dq^2}{dt} \tag{4}$$

and decreases with increasing x/M. Friehe and Schwarz[11] were able to collapse all of their grid turbulence data onto a single curve through the use of Eq. (4).

Using Eq. (1), the definitions of ϵ and q, and $n=1.3$, one has

$$\epsilon M/(q^2U)=0.65(x/M)^{-1} \tag{5}$$

$$\epsilon M/U^3=0.0865(x/M)^{-2.3} \tag{6}$$

The turbulence parameter ϵ^*, defined by Crow and Bate[15] as

$$\epsilon^*=(\epsilon b_0)^{1/3}/V_0 \tag{7}$$

may be combined with Eq. (6) to yield

$$\epsilon^*=\frac{1}{(V_0/U)}\frac{0.4423}{(M/b_0)^{1/3}}\left(\frac{x}{M}\right)^{-0.767} \tag{8}$$

in which M/b_0 represents the ratio of the mesh size to the initial vortex separation. The values of V_0/U and M/b_0 are known for a given grid and model. The exact value of A_1 [0.05 in Eq. (2)] is not critical. It is easy to show that a change even as large as 20% in A_1 (say, from 0.05–0.06) causes only a 6% change in ϵ^*.

The integral scale L_{11} of the grid-generated turbulence field has been measured by a number of investigators.[9-14] The results have shown that L_1 increases with x/M. Huot et al.[14] found experimentally that L_{11}/M may be represented by

$$L_{11}/M=0.14(x/M-x_0/M)^{0.4} \tag{9}$$

in which x_0/M represents the distance to a fictitious origin. For the grid size used in the present experiments, x_0/M is about 2.5. However, it is not necessary to retain x_0/M in Eq.

(9) simply because in the present experiments x/M ranged from a minimum value of 50 to about 1000. Thus, one has

$$L_{11}/b_0 = 0.14(M/b_0)(x/M)^{0.4} \quad (10)$$

Equation (10) shows that L_{11}/b_0 is about 1.57 for the smaller model (N-2 with $M/b_0 = 0.707$) and about 1.0 for the larger model (N-1 with $M/b_0 = 0.47$). Thus, it is seen that the integral scale of the turbulence generated by the grid used in the present experiments varies from one half to 1.5 times the initial vortex separation. In other words, it is within the distances cited that the integral scale of the background increases and becomes comparable to the size of the individual vortices.

Test Procedures

A model is attached to the bottom carriage at the desired angle of attack (-6 to -12 deg) and filled with neutrally buoyant fluorescent dye to seed the vortex cores. Then the basin is filled gradually with fresh water to the desired level ($d_0/b_0 > 8$). After removal of trapped air and after a sufficient period of waiting for the escape of dissolved air in the water and the elimination of any internal currents in the basin, the grid is set in motion at the desired speed. When the grid has moved a prescribed distance of x/M, the model was set in motion. As noted earlier, the grid and the model moved at identical speeds, i.e., the horizontal distance between them was kept constant at a given value of x/M. Most of the experiments were repeated at least three times.

Vortex trajectories were visually observed and recorded on high-speed Polaroid film and on video tape at the test section (one of the plexiglass panels near the middle of the basin). Each picture included two clocks accurate to 0.1 s, the vertical and horizontal scales on the plexiglass window and, of course, the side view of the trailing vortices as they rose from the model after formation. The time interval between successive pictures is determined from the two clocks. The first picture always captured the instant the grid arrived at the test section. The second picture captured the instant the model passed through the test section. The subsequent pictures (taken at about 0.75 s intervals) captured the rise and demise of the vortices. The vertical rise of the vortices is determined from the vertical scale. Attention has been paid to the fact that the vortices are farther away from the scale on the window and that the scale placed vertically in the middle of the test section does not exactly correspond to the scale marked on the window due to refraction and parallax. The necessary correction was made by photographing a scale placed in water in the middle of the test section together with the scale marked on the window. This resulted in a simple conversion table which enabled the actual position of the vortex to be determined from the scale reading on the photograph.

The results are normalized and plotted in terms of the governing parameters and compared with those obtained in the previous runs. Each experiment was repeated three times for most of the data presented herein. All trailing vortices were recorded on film until the time they have completely dissipated.

Dimensional Analysis

The dependent parameter of major importance is the instantaneous elevation of the vortex pair H. It may be expressed as a function of the following parameters[4]:

$$H = f(t, U, d_0, \rho, \nu, B, \mathcal{R}, \alpha, g, r_e, \epsilon, L_{11}) \quad (11)$$

in which t represents the time; U the velocity of the model; d_0 the initial depth of the vortex pair; ρ_0 the density of water; ν the kinematic viscosity of water; B the base width of the model; $\mathcal{R}$ the aspect ratio of the model; α the angle of attack of the model; g the gravitational acceleration; r_e an effective core radius, characterizing the effect of the wing-tip shape in addition to other wing parameters; ϵ the rate of decay of the turbulent energy per unit mass; and L_{11} the integral scale of the turbulent field. The height and width of the test section and the height of the model within it were not included in the foregoing because a detailed analysis, based on ideal vortices, has shown that the wall and free-surface proximity effects were negligible. A dimensional analysis of Eq. (11) yields

$$H/B = f(Ut/B, d_0/B, U^2/gB, UB/\nu, \mathcal{R}, \alpha, r_e/B, \epsilon^*, L_{11}/b_0) \quad (12)$$

Equation (12) may be recast in terms of the initial separation b_0 of the vortex pair, and the initial mutual induction velocity V_0 of the vortices by noting that B/b_0 and V_0/U are uniquely determined by $\mathcal{R}$ and α for a given wing shape. Thus, one has

$$H/b_0 = f(V_0 t/b_0, d_0/b_0, V_0^2/gb_0, V_0 b_0/\nu, r_e/b_0, \epsilon^*, L_{11}/b_0) \quad (13)$$

Experiments have shown that[4] the ratio of the initial vortex-core spacing to wing span, b_0/B, is nearly equal to $\pi/4$ for the rectangular wings with rounded edges (NACA 0012).

The measurements have shown that[4] the dimensionless parameters V_0^2/gb_0 (a Froude number which ranged from 3×10^{-3} to 3×10^{-2}) and $V_0 b_0/\nu$ (a Reynolds number which ranged from 3500 to 10,500) are not important within the range of the parameters encountered in the present experiments. Furthermore, d_0/b_0 was kept larger than eight so as to eliminate or minimize the free-surface-proximity effects. Previous experiments[4] have shown that the vortices in homogeneous medium do not rise larger than about $6b_0$.

The core measurements were made at angles of attack of -8 and -12 deg and at model velocities of $U = 0.8$–4 ft/s, at a distance of 10 chord lengths downstream from the model. The diameter of the dye column was taken as the initial effective core size. It represented the region containing vorticity, save for the effect of the diffusion of dye over a distance of 10 chord lengths. The relationship between this core definition and others, such as the point of maximum velocity or a defini-

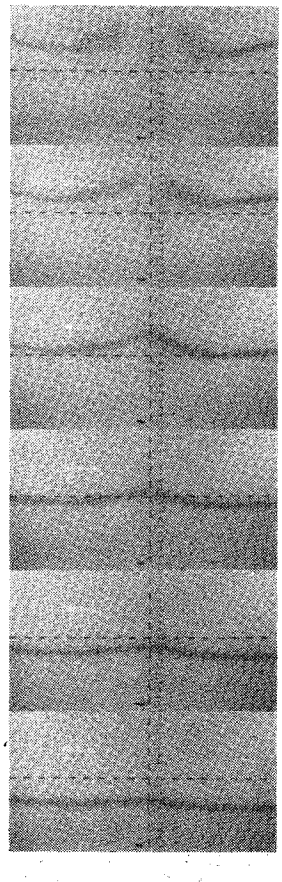

Fig. 2 Sinusoidal (Crow[1]) instability.

tion based on equivalent energy in the vortex,[16] cannot be deduced from these measurements.

The average of at least five measurements per model yielded $r_e/b_0 = 0.09 \pm 0.01$. The model speed and the angle of attack did not have a measurable effect on r_e/b_0. Admittedly, it is very difficult to obtain a precise measurement of r_e and to account for the diffusion of dye over a time period of 10 c/U (0.5–3 s). However, in all cases, r_e did not differ more than about 12% from the average of over five measurements per model.

With the foregoing arguments, Eq. (13) may be written as

$$H^* = f(T^*, \epsilon^*, L_{11}/b_0) \tag{14}$$

where $H^* = H/b_0$. The other parameters have been defined previously.

Discussion of the Results

In a quiescent or weakly turbulent medium ($\epsilon^* < 0.05$), the sinusoidal instability (thought to be driven by the turbulence generated in and by the vortex cores) develops slowly at first and then rapidly as shown in Fig. 2. According to Crow,[1] the instability grows by a factor e in a time 1.21 b_0/V_0 in fixed planes which are inclined to the horizontal at an angle of about 48 deg. The most unstable mode has a wavelength of $8.6b_0$ (assuming $r^* = 0.098$ and a uniform vorticity distribution in the core[16]). When the vortices link, a series of vortex rings of highly complex shapes develops. The rings continue to rise for a while and then completely dissipate.

At larger values of ϵ^* (>0.1), a cascade of core bursts (sometimes referred to as the vortex breakdown) occurs on one or both of the vortices. The bursts are neither equally spaced nor at the same axial location along each vortex (i.e., not adjacent pairs). Furthermore, the bursts remain stationary (see Fig. 3) and the vortex filaments upstream and downstream of a burst remain practically unaffected. These observations are in contradiction to those made on single vortices in a tube.[17] In other words, the core bursting in trailing vortices does not signal a transition from supercritical to subcritical flow. The causes and the structure of the bursts remain unknown. The vortices survive the core bursting and continue to rise before they are completely dissipated by subsequent instability events. One notable exception to the foregoing is that occasionally the core bursting occurs on only one of the vortices. Then that vortex is rapidly destroyed while its mate remains stable and continues to rise for an additional period of about $V_0 t/b_0 = 1 \sim 2$. Similar observations were made by Tombach[7] on vortices generated by an aircraft.

In the range of $0.05 < \epsilon^* < 0.1$, either sinusoidal instability or core bursting occurred. The sinusoidal instability did not result in linking. In fact, the distance between the vortices often increased and the plane of vortices rolled to a near vertical position. The rolling motion was also observed at higher levels of turbulence prior to the occurrence of core bursting (see Fig. 4). The direction of the roll motion along the vortex pair changed, i.e., there was no dominant direction. Thombach[7] also noted that the vortex system rolled up onto its side at all levels of stability and turbulence. He suggested that atmospheric shear may be the cause of roll. The present experiments suggest that shear is not necessary for the roll. As one would expect, the lateral and vertical displacements of the vortices are controlled by the magnitude and sense of the turbulent velocity components in the respective directions. Thus, the lateral and vertical separation of the vortices may be increased or decreased depending on the sense of the velocities in the respective directions. An increased or decreased lateral separation with increased vertical separation will result in a roll motion. The direction of roll may be clockwise or counterclockwise, as shown by the present observations. In their calculation of the lifespan of trailing vortices in strong turbulence, Crow and Bate[15] considered only the lateral displacement of the vortices, as will be discussed in more detail later.

Figures 5 and 6 show H^* vs T^* for $x/M = 750$ ($\epsilon^* = 0.13$) and $x/M = 250$ ($\epsilon^* = 0.31$), respectively. The full circles in Fig. 6 are for a vortex which continued to rise after the destruction of its mate due to a cascade of core bursts. These figures show that the migration of the vortex pair deviates gradually at first and then rapidly (at $T^* = 3$ in Fig. 5 and at $T^* = 1.3$ in Fig. 6) from the ideal line ($H^* = T^*$) and that the maximum height at-

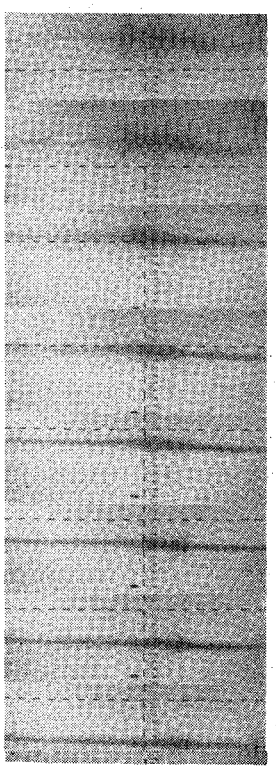

Fig. 3 Vortex core bursting.

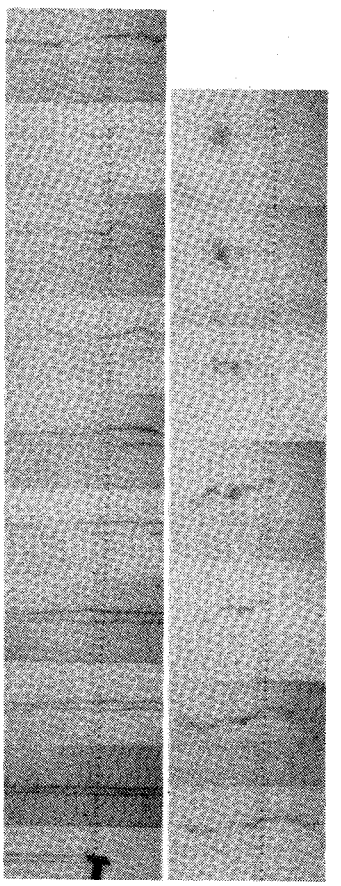

Fig. 4 The roll of the vortices and core bursting (up and then to the right).

tained by the vortices decreases with increasing ϵ^* (decreasing x/M). The time at which the rapid change in the slope of the mean line through the data occurs corresponds to the time at which the core bursting occurs. The vortices continue to rise for an additional time of $\Delta T^* = 1.7$ in Fig. 5 and $\Delta T^* = 0.5$ in Fig. 6 until they are finally destroyed by the subsequent instability events. The stronger the ambient turbulence the shorter is the time between the onset of core bursting and final destruction. The scatter in the data is partly due to the fact that the vortex pair does not deform or demise in a similar manner from one test to another. The three-dimensional nature of the ambient turbulence, the rotation of the pair along a horizontal axis, sinusoidal instability, and the occasional occurrence of core bursting in only one of the vortex pair change the relative positions of the vortices at the test section and give rise to some scatter in the data. It is rather remarkable that the scatter is not any larger.

Figure 7 is a composite plot of the mean lines through the data for representative values of x/M. Evidently, the ambient turbulence plays a profound role in the destruction of the vortices. For x/M smaller than about 500 ($\epsilon^* < 0.18$), the vortices rise only a distance of b_0 to 1.5 b_0 before they are destroyed.

For the grid used in the tests, L_{11}/b_0 decreased from 0.93 at $x/M = 750$ to 0.52 at $x/M = 180$ for the model N-1 and from 1.4 at $x/M = 750$ to 0.8 at $x/M = 180$ for the model N-2 [see Eq. (10)]. Thus, L_{11}/b_0 for the model N-1 is comparable to the initial separation distance of the vortices for x/M larger than about 750. The same is true for the model N-2 for x/M between 250 ($L_{11}/b_0 = 0.9$) and 500 ($L_{11}/b_0 = 1.2$).

It appears that strong turbulence with small integral scale (small x/M) leads to the eventual deposition of vorticity in larger and larger regions of the vortex without the more dramatic and destructive effects of larger scale motions. On the other hand, weaker turbulence with larger integral scale (larger x/M) leads to strong instabilities, breaks up the vortices and leaves them in a state to be devoured by small intensity turbulence. Subsequently, the vorticity is diffused outward and finally destroyed completely. It is clear from the foregoing that the lifespans of the vortices depend significantly on the intensity of turbulence and to a lesser extent on its scale. The quantification of the effect of integral scale is not yet possible. However, the data obtained in the present investigation with two models and two grids strongly suggest that the relationship between H^* and T^*, the maximum height attained by the vortices and the lifespan of the vortex pair are governed primarily by ϵ^*.

Figure 8 shows the maximum height data obtained with both models as a function of ϵ^*. Also shown in this figure is the flight data obtained by Tombach.[7] There is reasonable agreement between the laboratory and flight data in spite of the considerable scatter due to the difficulty of determining the maximum height attained by the vortices. As noted earlier, the uncertainties stem partly from the randomness in the occurrence of the instabilities and partly from the experimental difficulties and uncertainties (diffusion of dye, subjectivity in deciding the exact position of the vortex core, etc.). It appears that ϵ^* is the primary governing parameter in the determination of the maximum height. The role of the integral scale is not clearly discernable and is partly obscured by the scatter in the data.

Figure 9 shows the lifespan [T^*(max)] of the vortices as a function of ϵ^*. The data points shown near the T^* axis correspond to the no-turbulence case. It is assumed that the effect of turbulence is negligible for ϵ^* smaller than about 0.01 in order to show the entire data in the figure. Clearly, the effect of turbulence is to reduce both the lifespan and the maximum height attained by the vortices. Despite large differences in Γ/ν and the integral scale of turbulence, the data agree surprisingly well with those of Tombach[7]. This fact further reinforces the assertion that the scale effects (Reynolds number and integral scale) play at best relatively minor roles and that the migration and demise of the vortices in a turbulent environment are controlled primarily by the turbulence parameter ϵ^*.

Also shown in Fig. 9 (dashed line) is the lifespan expression

$$\epsilon^* = 0.87 T^{*1/4} \exp(-0.83 T^*) \tag{15}$$

obtained by Crow and Bate[15] for weak turbulence. Equation (15) is valid only in the region where ambient turbulence leads to sinusoidal instability, i.e., for ϵ^* less than about 0.1. For an environment with strong turbulence, Crow and Bate[15] obtained

$$T^* = 0.41/\epsilon^* \tag{16}$$

Equation (16) is based on sinusoidal instability and considers only the lateral diaplacement of the vortices. Furthermore, the root-mean-square spacing of the vortices is assumed to be equal to the initial vortex separation. If the vortex displace-

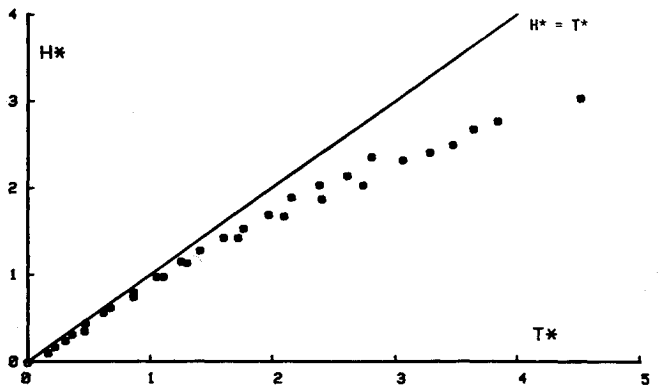

Fig. 5 H^* vs T^* for $x/M = 750$ (Model N-2).

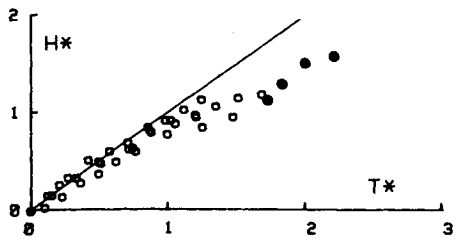

Fig. 6 H^* vs T^* for $x/M = 250$ (Model N-2).

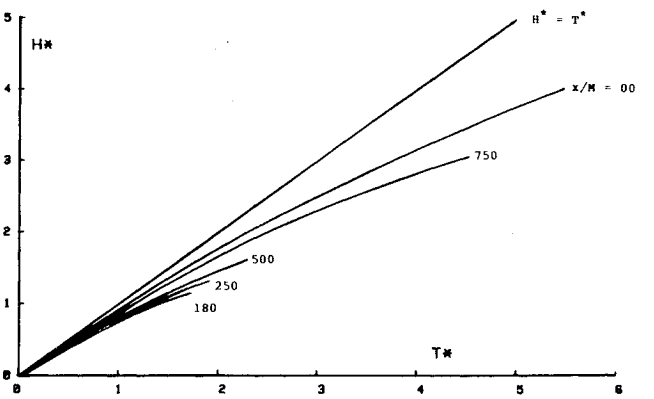

Fig. 7 H^* vs T^* for various representative values of x/M.

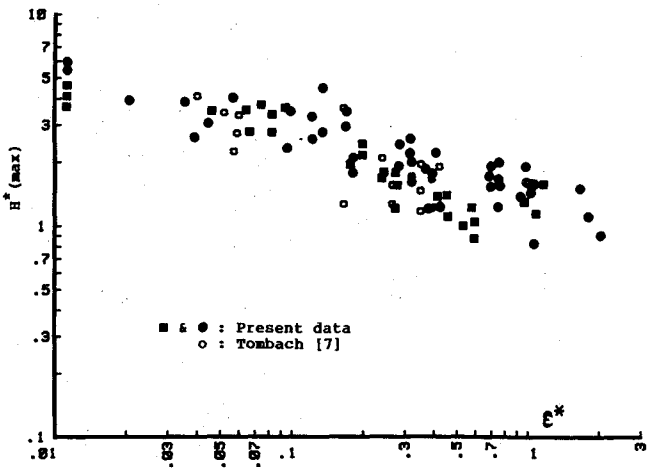

Fig. 8 H^*(max) vs ϵ^* for both models and Tombach's[7] aircraft data.

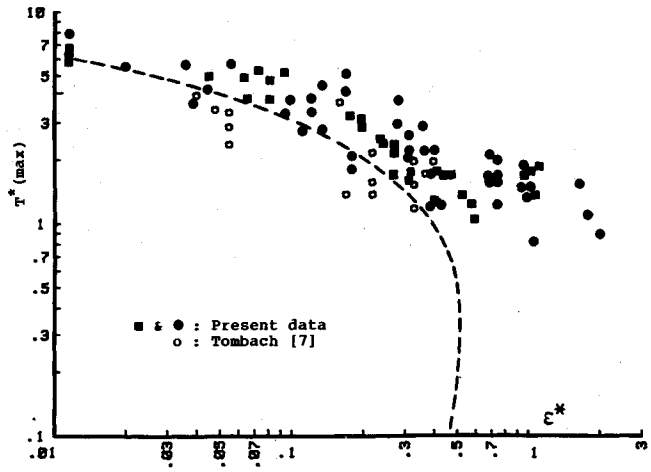

Fig. 9 T^*(max) vs ϵ^* for both models and Tombach's[7] aircraft data.

ments were considered to be nearly sinusoidal, the coefficient 0.41 in Eq. (16) would have reduced to 0.205. Consequently, the predictions of Eq. (16) for the strong turbulence would have fallen considerably below the experimental data. The fact that the dominant instability in strong turbulence is vortex bursting and that the analysis of Crow and Bate[15] does not deal with this instability, Eq. (16) is inappropriate for the prediction of the lifespan of vortices in strong turbulence. It is for this reason that Eq. (16) is not plotted in Fig. 9.

Conclusions

The investigation reported herein has shown that the effect of ambient turbulence in homogeneous medium is to inhibit the migration and the lifespan of the vortices. In weak turbulence, sinusoidal instability and the subsequent instability events destroy the vortices. In medium to strong turbulence, the dominant form of instability is the vortex bursting. The reasons leading to the occurrence of a cascade of core bursts often in both vortices and occasionally in one vortex remain unknown. The vortices do not remain in a horizontal plane but roll about each other. Thus, shear is not necessary for the roll. However, the roll may be enhanced by shear in aircraft wakes. The migration and the lifespan of the vortices appear to be governed primarily by the turbulence parameter ϵ^*. The agreement between the present data (for two models and grids) and the field data strongly suggests that the integral scale of turbulence is of minor importance. The core bursting and its role in the demise of the trailing vortices need further experimental and theoretical work.

Acknowledgments

The work described herein was part of a larger program which included the experimental and numerical investigation of trailing vortices in homogeneous and density stratified media. The continued support of the Defense Advanced Research Projects Agency (DARPA) is sincerely appreciated.

References

[1]Crow, S. C., "Stability Theory of a Pair of Trailing Vortices," *AIAA Journal*, Vol. 8, Dec. 1970, pp. 2172–2179.

[2]Windnall, S. E., "The Structure and dynamics of Vortex Filaments," *Annual Review of Fluid Mechanics*, Vol. 7, 1975, pp. 141–165.

[3]Hecht, A. M., Bilanin, A. J., Hirsh, J. E., and Snedeker, R. S., "Turbulent Trailing Vortices in Stratified Fluids," *AIAA Journal*, Vol. 18, July 1980, pp. 738–746.

[4]Sarpkaya, T., "Trailing Vortices in Homogeneous and Density-Stratified Media," *Journal of Fluid Mechanics*, Vol. 136, 1983, pp. 85–109.

[5]Greene, G. C., "An Approximate Model of Vortex Decay in the Atmosphere," *Journal of Aircraft*, Vol. 23, July 1986, pp. 566–573.

[6]Burnham, D. C., Hallock, J. N., Tombach, I. H., Brashears, M. R., and Barber, M. R., "Ground Based Measurements of a B-747 Aircraft in Various Configurations," U.S. Dept. of Transportation Rept. FAA-RD-78-146, 1978.

[7]Tombach, I., "Observations of Atmospheric Effects on Vortex Wake Behavior," *Journal of Aircraft*, Vol. 10, Jan. 1973, pp. 641–647.

[8]Sarpkaya, T. and Daly, J. J., "Effects of Ambient Turbulence and Stratification on the Demise of Trailing Vortices," Naval Postgraduate School, Monterey, CA, Tech. Rept. NPS69-86-006, 1986.

[9]Compte-Bellot, G. and Corrsin, S., "The Use of a Contraction to Improve the Isotropy of Grid-Generated Turbulence," *Journal of Fluid Mechanics*, Vol. 25, 1966, pp. 657–682.

[10]Compte-Bellot, G. and Corrsin, S., "Simple Eulerian Time Correlation of Full-and Narrow-Band Velocity Signals in Grid-Generated 'Isotropic' Turbulence," *Journal of Fluid Mechanics*, Vol. 48, 1971, pp. 273–337.

[11]Friehe, C. A. and Schwarz, W. H., "Grid-Generated Turbulence in Dilute Polymer Solutions," *Journal of Fluid Mechanics*, Vol. 44, 1970, pp. 173–193.

[12]Gad-el-Hak, M., "Experiments on the Nearly Isotropic Turbulence Behind a Jet Grid," Ph. D. Dissertation, Johns Hopkins University, Baltimore, MD, 1972.

[13]Schedvin, J. C., Stegen, G. R., and Gibson, C. H., "Universal Similarity at High Grid Reynolds Numbers," *Journal of Fluid Mechanics*, Vol. 65, 1974, pp. 561–579.

[14]Huot, J. P., Rey, C. and Arbey, H., "Experimental Analysis of the Pressure Filed Induced on a Square Cylinder by a Turbulent Flow," *Journal of Fluid Mechanics*, Vol. 162, 1986, pp. 283–298.

[15]Crow, S. C. and Bate, E. R. Jr., "Lifespan of Trailing Vortices in a Turbulent Atmosphere," *Journal of Aircraft*, Vol. 13, July 1976, pp. 476–482.

[16]Spreiter, J. R. and Sacks, A. H., "The Rolling-up of the Trailing Vortex Sheet and Its Effect on the Downwash Behind Wings," *Journal of Aerospace Sciences*, Vol. 18, 1951, pp. 21–23.

[17]Sarpkaya, T., "On Stationary and Travelling Vortex Breakdowns," *Journal of Fluid Mechanics*, Vol. 45, pp. 545–559.